TRANSPORTATION TECHNOLOGY CENTER, INC.
TECHNOLOGY DIGEST
JUNE 2021
TD21-012

The research described was performed by Transportation Technology Center, Inc., a wholly owned subsidiary of the Association of American Railroads.

Validation of In-Motion ECHO-Rail System for RCD Crack Depth Measurement

Anish Poudel and Matt Witte

Key Findings:

- The revised electronics in the Athena ECHO-Rail G3 sensor allowed for increased data sampling frequency as well as improved SNR performance.
- The G3 sensor achieved sustained data acquisition rates of at least 2,000 samples/second.

TTCI performed validation testing of the Athena Industrial Services Ltd. (Athena) ECHO-Rail Generation 3 (G3) sensor on track at the Rail Defect Test Facility (RDTF), Transportation Technology Center (TTC), Pueblo, CO. These tests were designed and performed using the TTCI rail inspection truck at various speeds with calibrated Electromagnetic Field Imaging (EMFI) sensor. In prior work,[1,2] Athena produced both an EMFI rail-shaped sensor and a calibration profile for the rail EMFI probe designed specifically for rail head inspection. Measurement data gathered during earlier tests was used to create a calibration curve and redesign of the contoured sensor. The primary goal of this work was to validate the calibration method developed in prior phases.

The phase detailed in this *Technology Digest* evaluated the readiness level of Athena's EMFI technology for future commercial deployment. During on-board testing, a new user interface (UI) was designed and the rail scanning application for storing, analyzing, and processing large, acquired data sets were applied. Data acquisition at speeds up to 20 mph was demonstrated in Phase 2 work.[2] Improved control electronics for the EMFI probe along with the calibrated data analysis algorithms provided defect depth measurements while compensating for the effects of changes in rail head profile and rail metallurgy. Testing was performed at speeds of 4, 8, and 12 mph on track at the RDTF.

SENSOR REDESIGN AND CONFIGURATION

The EMFI sensor is non-contact, and operates at about 0.5-inch offset from the rail head. For this phase, Athena revised and redesigned their EMFI sensor electronics to improve the maximum data sampling speed and the signal-to-noise ratio (SNR) performance of the magnetic field sensing circuits. When combined with improvements in the magnetic field position analysis algorithms, the scanning speed capability in this phase increased by 340 percent with an 80 percent reduction in SNR as compared to the results obtained in prior phases. For example, the Generation 2 (G2) sensor used during Phase 2 work[1,2] was only capable of 450 samples/second.

Sustained data acquisition rates of at least 2,000 samples/second were achieved by the G3 sensor used during this phase of work. Further, the electronics packaging optimization allowed the rail-shaped sensor used in this phase, to be self-contained; thereby requiring only power, odometer, and USB connections. Urethane potting of the sensor system served to protect against both environmental and physical damage. Physically, the form factor of the revised packaging increased in height by approximately 0.5 inch, and the sensor assembly was mounted in the same high rail carriage that was used in the prior work.[2] Figure 1 shows the EMFI rail-shaped sensor on the TTCI rail inspection truck.

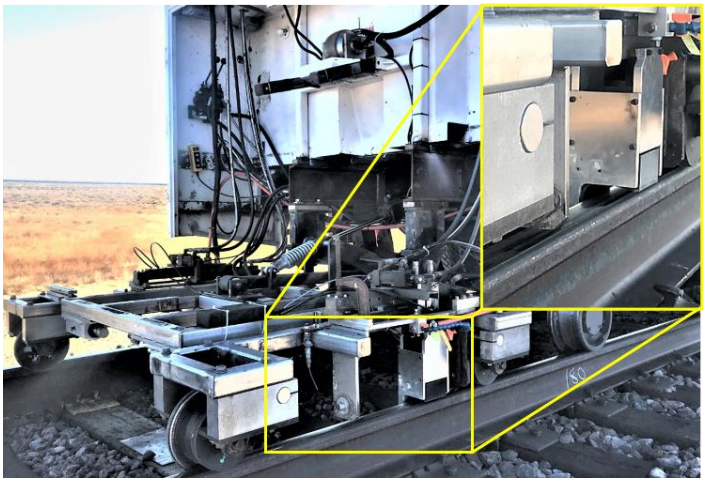

Figure 1. Non-contacting EMFI rail-shaped sensor on TTCI inspection truck

SENSOR CALIBRATION

Data acquired during earlier phases at TTC produced calibration reference values that were applied to the G3 sensor. Based on the previous testing and experiences, it was determined that four primary factors influenced the calibrated RCD results:

- **Local and extended variations in the rail head profile:** When comparing the rail under test to the reference rail, these variations cause significant baseline data value changes. The revised profile compensation algorithm was applied to the sensor.
- **Metallurgical variations between the rail under test and the reference rail:** These variations typically affect the accuracy of crack depth measurement. The effects of metallurgical variation, particularly magnetic permeability, are a fundamental cause of inconsistent results from other forms of electromagnetic-based technology. A processing method was developed that utilized EMFI field density data to compute a defect depth correction factor.
- **Defect density:** Characterized as the number of defect events per inch or mm, the defect density affects signal magnitude. Defect density correction algorithms were modified and applied to the data analysis presented.
- **Ride stability**: This refers specifically to the stability of the sensor carriage that runs on the rail surface. Instabilities in the 1Hz–30Hz range can affect the quality of acquired data. During the test, trolley instability appeared to become significant at speeds over 8 mph. Observations made during the test run, in addition to data artifacts present at the rail joints, seemed to indicate that the chassis movement of the hi-rail vehicle was being coupled into the trolley. Rapid trolley movements caused sensor responses that looked like large crack events.

TEST SETUP AND CONFIGURATION

Field testing took place at the RDTF on a segment with replaceable rail. The test rails installed for this study were high and low rail sections that were retrieved from the Section 7 curve of the High Tonnage Loop (HTL) at TTC. Both test rails were installed in the same side of the track and were positioned end-to-end and ground over a short distance to transition the rail head profiles. The high rail was about 27-feet long and the low rail was about 39 feet long. RCD visual ratings for these rails varied from 1 to 2. RCD visual ratings for the rail is described in prior TTCI work.[3] Measurement locations were selected every fourth tie. There were four measurement locations in the high rail and five measurement locations in the low rail. These test rails were also characterized by taking both MiniProf rail profile and liquid dye penetrant (PT) measurements at each measurement position. Test runs were made at speeds of 4, 8, and 12 mph, and data was analyzed immediately after all of the runs. Based on the aggregate data, a grind depth was determined and the rails were ground accordingly. The goal was not to remove the RCD cracks completely during the grinding, but to leave the cracks behind for comparison and validation of the post-grind EMFI measurements with the destructive analysis.

After the grind, EMFI measurements were repeated at various speeds. Post-grind Miniprof and PT measurements were also taken, and the rails were removed for destructive testing, which involved sectioning the rails and examining the cracks and pits at each measurement location.

RESULTS

The contoured sensor acquired data from multiple antennas within the probe. These antennae were located across the running surface of the rail from the field corner to the gage face. Data loss was observed at 8 and 12 mph. This loss was traced to signal quality degradation from the distance encoder on the hi-rail test vehicle. This degradation in quality was mainly attributed to the difference in the wiring of the encoder: the data acquisition system for the EMFI sensor hardware was wired as a single-ended encoder; whereas, the truck encoder was a differential encoder. As a result of the encoder incompatibility and resulting signal quality degradation, the incoming data was not sampled correctly at higher speeds. Therefore, the results presented in this report are only for the 4-mph test runs.

Figure 2 shows the pre-grind EMFI output for the test rails at 4 mph. The X-axis is the traveled distance and Y-axis is the defect severity (arbitrary value). The full-scale events at the beginning, middle, and the end correspond to carriage vertical motion on the bolted joint transitions. Also, the effect of trolley instability was apparent near these bolted rail joints, and the instability persisted for approximately 20 inches before and after the joint.

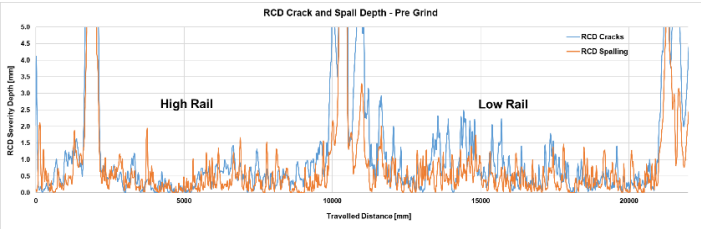

Figure 2. Pre-grind crack and spall depth maximal values for test rails

These distances are consistent with the spacing of the steel high rail wheels and the steel wheels on the carriage. The data is stable and of good quality in the areas between the jointed transitions. The values between these transitions represent maximum crack depth in that interval. From this data, it can be determined that a grinding depth of 1.5 mm should remove most of the defects in both rails. There should still be some residual cracks measuring between 0.5 and 1 mm remaining in the low rail with a 1.5-mm grind depth. It is also expected that some small amount of spalling will remain. Based on this pre-grind EMFI measurement, it was determined to grind 1 mm.

Figure 3 compares the pre- and post-grind rail profile comparisons taken at Location 4 using Miniprof.

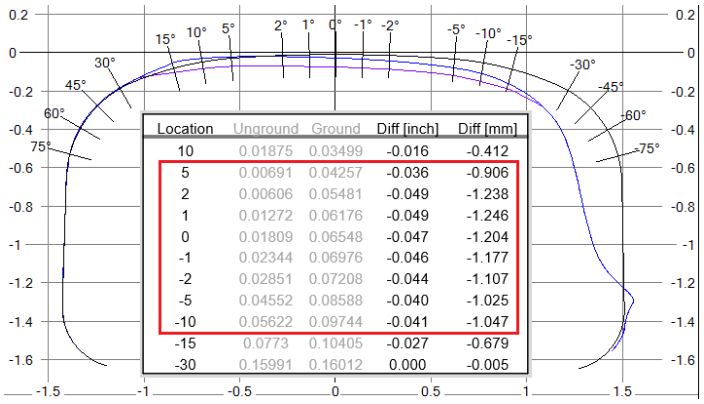

Location	Unground	Ground	Diff [inch]	Diff [mm]
10	0.01875	0.03499	-0.016	-0.412
5	0.00691	0.04257	-0.036	-0.906
2	0.00606	0.05481	-0.049	-1.238
1	0.01272	0.06176	-0.049	-1.246
0	0.01809	0.06548	-0.047	-1.204
-1	0.02344	0.06976	-0.046	-1.177
-2	0.02851	0.07208	-0.044	-1.107
-5	0.04552	0.08588	-0.040	-1.025
-10	0.05622	0.09744	-0.041	-1.047
-15	0.0773	0.10405	-0.027	-0.679
-30	0.15991	0.16012	0.000	-0.005

Figure 3. Grind depths determined using Miniprof at Location 4

Figure 4 shows the overlay plot for the pre- and post-grind RCD crack depth measurements. The black solid lines indicate the location where other measurements (MiniProf and PT) were taken.

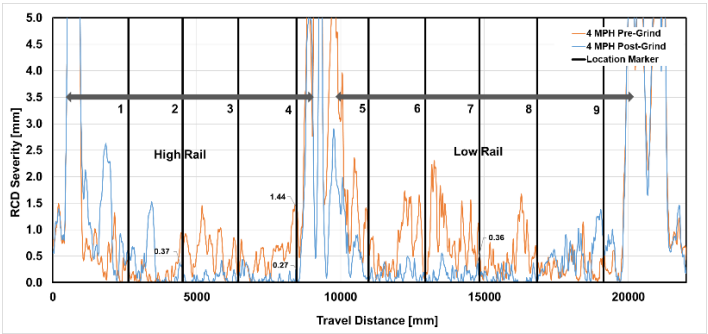

Figure 4. Pre- and post-grind EMFI RCD crack depth severity measurement

In the figure, two additional responses are visible at approximately 2,200 mm and 3,900 mm in the post-grind data. Visual examination of the rail in these areas showed an irregular grind profile. In addition, the remaining crack depth indications after grinding appeared to be shallower than expected in the areas of high crack density. Visual inspection of the post-grind area showed that the defect density in these areas was significantly less than it was for the pre-grind test. While this result was expected, the visual examination also

revealed that the depth of the remaining crack defects appeared to be deeper than was indicated in Figure 4.

Subsequent evaluation of both the pre- and post-grind crack data showed that defect density appeared to provide a reasonable method for determining a crack depth correction factor for sparse cracking. A low-pass filtering approach was applied to make the graph more readable to foster a better understanding of the grind profiles. Figure 5 shows the revised post-grind crack depth analysis based on the low-pass filtering.

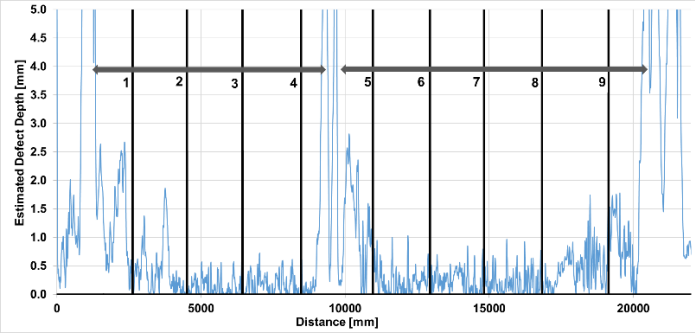

Figure 5. Post- grind running surface estimated crack depth measurement with low-pass filter applied

Figure 6 shows the pre- and post-grind visual and PT measurements for Location 4. Microscopy analysis was also conducted in order to determine the crack depth at the profile measurement locations. Figure 7 shows the deepest crack remaining at Location 4 after grinding, approximately 0.2 mm; which corresponds well with Figure 5.

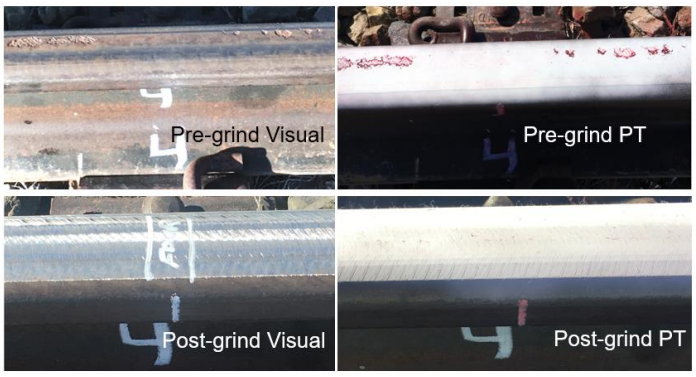

Figure 6. Pre- and post-grind visual and PT measurement for Location 4

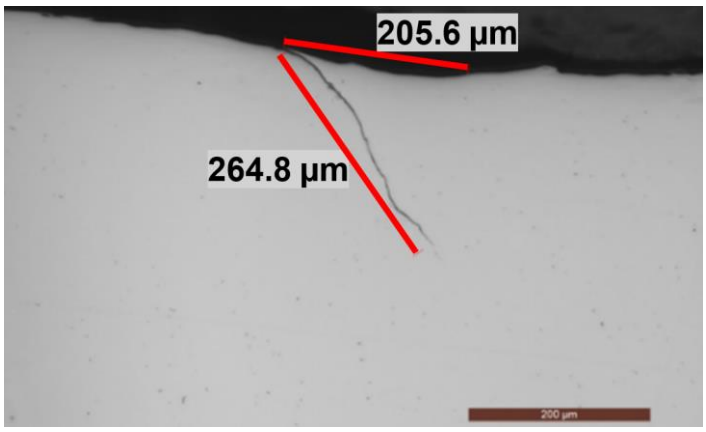

Figure 7. Post-grind micrograph near top of rail at Location 4

CONCLUSIONS

Calibrated and corrected data analysis algorithms demonstrated a good correlation to the defect depth measurements as verified by descructive testing. Methods of compensating for the effects of the changes in rail head profile and rail metallurgy were included in the analysis. This testing showed the need for additional revisions to the processing algorithm that corrects for the aggregate effects of defect density. These findings were significant when comparing pre- and post-grind scan results. The data analysis algorithms have not been developed to the point where the effects of platform instability can be removed.

References

1. Witte, M. W. and A. Poudel. July 2018. "Measuring Rolling Contact Damage in Rails Using EMFI." *Technology Digest* TD18-016. AAR/TTCI. Pueblo, CO.
2. Poudel, A. and M. W. Witte. May 2020. "Evaluation of In-Motion ECHO-Rail RCD Measurement System." *Technology Digest* TD20-007. AAR/TTCI. Pueblo, CO.
3. Banerjee, A. and D. D. Davis. February 2016. "FAST Premium Rail Wear Test Results: 2014-2015." *Technology Digest* TD16-001. AAR/TTCI. Pueblo, CO.

For comments or questions about this publication, contact
Anish_Poudel@aar.com